

The inflammation-resolution promoting molecule resolvin-D1 prevents atrial proarrhythmic remodelling in experimental right heart disease

Roddy Hiram ¹, Feng Xiong^{1,2}, Patrice Naud¹, Jiening Xiao¹, Martin Sirois¹, Jean-François Tanguay¹, Jean-Claude Tardif ¹, and Stanley Nattel ^{1,2,3,4*}

¹Department of Medicine, Montreal Heart Institute (MHI), Université de Montréal, 5000 Belanger Street, Montreal, QC H1T 1C8, Canada; ²Department of Pharmacology and Therapeutics, McGill University, Montreal, QC, Canada; ³IHU Liryc and Fondation Bordeaux Université, Bordeaux, France and ⁴Institute of Pharmacology, West German Heart and Vascular Center, Faculty of Medicine, University Duisburg-Essen, Essen, Germany

Received 4 March 2020; revised 16 June 2020; editorial decision 22 June 2020; accepted 24 August 2020; online publish-ahead-of-print 31 August 2020

Time for primary review: 25 days

Aims

Inflammation plays a role in atrial fibrillation (AF), but classical anti-inflammatory molecules are ineffective. Recent evidence suggests that failure of inflammation-resolution causes persistent inflammatory signalling and that a novel drug-family called resolvins promotes inflammation-resolution. Right heart disease (RHD) is associated with AF; experimental RHD shows signs of atrial inflammatory-pathway activation. Here, we evaluated resolvin-therapy effects on atrial arrhythmogenic remodelling in experimental RHD.

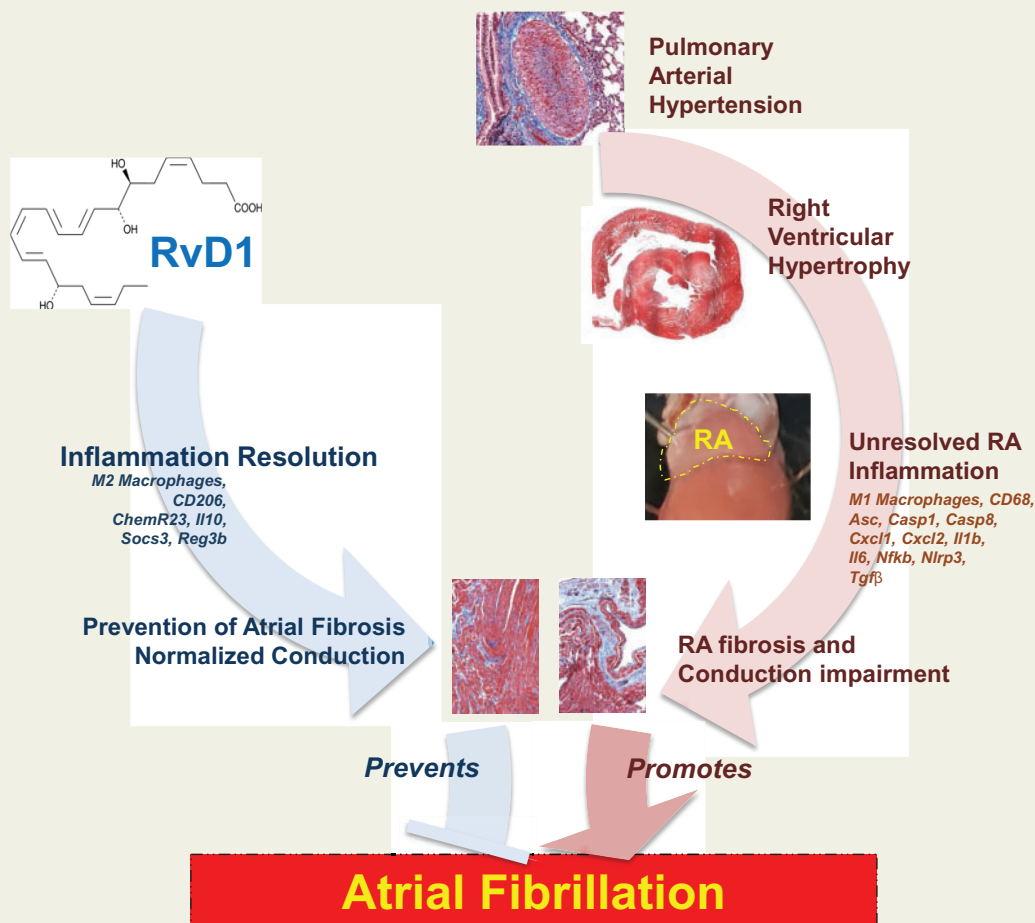
Methods and results

Pulmonary hypertension and RHD were induced in rats with an intraperitoneal injection of 60 mg/kg monocrotaline (MCT). An intervention group received daily resolvin-D1 (RvD1), starting 1 day before MCT administration. Right atrial (RA) conduction and gene-expression were analysed respectively by optical mapping and qPCR/gene-microarray. RvD1 had no or minimal effects on MCT-induced pulmonary artery or right ventricular remodelling. Nevertheless, *in vivo* transoesophageal pacing induced atrial tachyarrhythmias in no CTRL rats vs. 100% MCT-only rats, and only 33% RvD1-treated MCT rats ($P < 0.001$ vs. MCT-only). Conduction velocity was significantly decreased by MCT, an effect prevented by RvD1. RHD caused RA dilation and fibrosis. RvD1 strongly attenuated RA fibrosis but had no effect on RA dilation. MCT increased RA expression of inflammation- and fibrosis-related gene-expression pathways on gene-microarray transcriptomic analysis, effects significantly attenuated by RvD1 (334 pathways enriched in MCT-rats vs. control; only 177 dysregulated by MCT with RvD1 treatment). MCT significantly increased RA content of type 1 (proinflammatory) CD68-positive M1 macrophages without affecting type 2 (anti-inflammatory) M2 macrophages. RvD1-treated MCT-rat RA showed significant reductions in proinflammatory M1 macrophages and increases in anti-inflammatory M2 macrophages vs. MCT-only. MCT caused statistically significant increases in protein-expression (western blot) of COL3A1, ASC, CASP1, CASP8, IL1 β , TGF β 3, CXCL1, and CXCL2, and decreases in MMP2, vs. control. RvD1-treatment suppressed all these MCT-induced protein-expression changes.

Conclusion

The inflammation-resolution enhancing molecule RvD1 prevents AF-promoting RA remodelling, while suppressing inflammatory changes and fibrotic/electrical remodelling, in RHD. Resolvins show potential promise in combating atrial arrhythmogenic remodelling by suppressing ongoing inflammatory signalling.

Graphical Abstract



Caption: RvD1 attenuates AF vulnerability via inhibition of inflammation and fibrosis
 Pulmonary hypertension caused by monocrotaline leads to right ventricular hypertrophy and persistent, unresolved right atrial (RA) inflammation, which causes RA fibrosis, conduction abnormalities and an AF substrate. Treatment with resolvin D1 (RvD1) promotes resolution of RA inflammation, prevents fibrosis and suppresses development of the AF substrate.

Keywords

Arrhythmia • Atrial fibrillation • Fibrosis • Inflammation • Resolvin • Electrophysiology

1. Introduction

Right heart disease (RHD) is associated with structural and functional remodelling that promotes atrial fibrillation (AF), the most common cardiac arrhythmia.¹ AF is common in RHD associated with a range of common clinical conditions, including chronic obstructive pulmonary disease,² pulmonary arterial hypertension,³ and congenital cardiac disease⁴ and is associated with impaired outcomes.^{4,5} The mechanisms by which RHD promotes AF are poorly understood, and the therapeutic implications of these mechanisms are largely unknown.⁶

Atrial fibrosis is commonly associated with AF and is believed to play a significant pathophysiological role.^{1,7,8} We recently studied AF-promoting right atrial (RA) remodelling in an animal model of RHD

associated with monocrotaline (MCT)-induced pulmonary hypertension (PH) and found that conduction abnormalities caused by atrial fibrosis play a prominent role in the arrhythmogenic substrate.⁹ Furthermore, we obtained evidence pointing to inflammatory signalling as an important contributor to RHD-induced RA fibrosis.⁹

Chronic inflammatory signalling has been implicated as a pathogenic mechanism in a variety of cardiac conditions, including AF.^{10–13} An evolving concept in the area of chronic diseases is that there are discrete processes leading to the resolution of acute inflammation, and when these fail, chronic inflammation results, leading to chronic disease.^{14,15} It has been suggested that failed resolution of inflammatory processes (leading to chronicization of disease-promoting inflammation) can be ameliorated with the use of inflammation-resolution

promoting molecules.^{14,15} Recent studies have revealed that *n*-3 polyunsaturated fatty acid (PUFA)-derived immune response modulating compounds, including resolvins such as E Series molecules (abbreviated 'RvEs') derived from eicosapentaenoic acid (EPA) and D Series molecules ('RvDs') derived from docosahexaenoic acid (DHA), attenuate inflammation-related injury and its consequences in aortic, renal, pulmonary, cerebral, and ocular diseases.^{15–19} Evidence in cardiac disease is limited, but Halade *et al.*¹⁶ showed that RvD type-1 (RvD1) prevented cardiorenal syndrome after experimental myocardial infarction in mice.

Since we previously observed persistent activation of atrial inflammatory signalling in an RHD rat model 21 days after the initial insult,⁹ we considered the possibility that unresolved inflammation might be contributing to the pathophysiology of the RA substrate that promotes AF. We hypothesized that resolvins might suppress the development of the AF-promoting substrate associated with RHD by promoting the resolution of inflammation, and selected the autacoid and bioactive lipid pro-resolution molecule RvD1^{20,21} to study in the animal model of RHD. Accordingly, the objectives of the present study were: (i) to evaluate the effect of RvD1 on AF susceptibility due to RHD in the MCT-induced rat model of PH; (ii) to investigate the effect of RvD1 on arrhythmogenic RHD-induced atrial structural, functional and electrical remodelling; and (iii) to evaluate the impact of RvD1-therapy on the expression of underlying molecular pathways.

Methods

Animal model of RHD and RvD1 intervention

Experiments and animal handling procedures were approved by the Animal Ethics Committee of the Montreal Heart Institute and were conducted in accordance with the Canadian Council on Animal Care (CCAC) and NIH Guide for the Care and Use of Laboratory Animals. The approval reference number is 2016-2068, 2016-47-06. Adult male Wistar rats obtained from Charles River Laboratories (Montreal, Quebec) weighing 200–275 g were randomly assigned to each of four groups: control (vehicle-treated); control + RvD1; MCT; or MCT + RvD1. MCT rats received a single *i.p.* dose (60 mg/kg) of MCT. RvD1 treatment (2 µg/kg/day; *i.p.*) started 1 day before MCT injection. Control rats received an equivalent volume of vehicle (to MCT and RvD1). On Day 21 post-MCT injection, echocardiography, transoesophageal electrophysiological study (EPS), haemodynamic studies, and *ex vivo* optical mapping experiments were performed on six rats/group. For histological and biochemical analysis, six additional rats/group were euthanized with *i.p.* ketamine (100 mg/kg) and xylazine (10 mg/kg) followed by cardiac excision. Heart tissues were dissected and weighed; and then two-thirds of each tissue was fixed in formalin (10%) while one-third was homogenized and fast-frozen in liquid nitrogen for subsequent analysis. For echocardiographic studies, haemodynamic measurements and EPS, animals were anaesthetised with an inhaled mixture of 3% isoflurane and 1 L/min O₂ throughout the procedure.

Echocardiography

At baseline, Days 14 and 21, echocardiograms were obtained with a phased array 10S probe (4.5–11.5 MHz) in a Vivid 7 Dimension system (GE Healthcare UltrasoundHorten, Norway). Parasternal long-axis views were recorded to obtain M-mode echocardiographic measurements of left atrial (LA) and RA dimension at end-systole (LAD_s and RAD_s) and diastole (LAD_d and RAD_d); tricuspid annulus plane systolic excursion (TAPSE), tricuspid regurgitation, left ventricular (LV) and right ventricular (RV) wall thickness (LAW and RAW), dimensions (LVD and RVD); LV and RV ejection time (ET), ejection fraction, and pulmonary artery flow.

Transoesophageal stimulation

Transoesophageal EPS was performed with 4-Fr quadripolar catheters/2-mm interpolar distances (St. Jude Medical #401993). Atrial arrhythmia inducibility was assessed by applying 12 3-s 50-Hz pacing-bursts (pulse width 2 ms, 4× threshold current), separated by 2-s intervals.²² AF was defined as a rapid (>800 beats/min) irregular atrial rhythm. Atrial flutter (AFI) was defined as a regular atrial tachyarrhythmia at a cycle length between 600 and 800 b.p.m. AF and AFI inducibility were quantified based on the induction of arrhythmia episodes lasting for at least 1 s immediately after a pacing-burst. If an atrial arrhythmia lasting more than 2 s was induced by a burst, subsequent pacing was suspended to avoid interfering with the induced episode. AF duration was defined as the mean duration of all induced AF episodes. Recording and analysis of surface electrocardiogram (ECG) and catheter signals were performed with lox2 software (version 2.8.0.13, EMKA technologies, FR).

Haemodynamic measurements

RV systolic pressure (RVSP) was measured with a 2-Fr pressure-transducer catheter (SPR 407 Pressure-only catheter, Mikro-Tip[®], ADInstrument, Colorado, USA) introduced via the right jugular vein. Recording and analysis of haemodynamic data were performed with lox2 software.

Optical mapping

The heart was excised and perfused via the aorta with Krebs solution at 10 mL/min and 37°C, containing (mM): NaCl 120, KCl 4, MgSO₄ 1.2, KH₂PO₄ 1.2, NaHCO₃ 2.5, CaCl₂ 1.25, D-Glucose 5.5. The Krebs solution was adjusted to pH 7.5 and bubbled with 95%-O₂/5%-CO₂. After 20 min for stabilization, mechanical contraction was suppressed using a recirculating solution of 15-µM blebbistatin. Di-4-ANEPPS (10 µM, 0.1 mL) was injected via the perfusate to detect voltage-fluorescence signals. Recordings were obtained at 2 kHz with a charge-coupled device camera (CardioCCD, RedShirtImaging, Decatur, GA, USA) focused on a region of up to approximately 8 × 8 mm (depending on the anatomy) in the RA or LA free wall. Effective refractory period (ERP: the longest S1–S2 coupling interval failing to generate a propagated beat) was determined with programmed stimulation at an S1S1 basic cycle length (BCL) of 150 ms followed by a decremental S2 extrastimulus beginning with an S1–S2 of 80 ms. Optical maps were then obtained over a range of BCLs (between 150 and 60 ms; 3 s each). *In situ* AF induction was performed over a range of BCLs between 300 and 60 ms, with 3-s bursts at each. Finally, 25-Hz burst pacing was applied as six repeated 3-s burst cycles separated by 1-s intervals, with burst-pacing suspended if AF-episodes occurred to avoid interfering with the evolution of the induced arrhythmia. Conduction velocity (CV) and action potential duration to 80% repolarization (APD₈₀) were measured with a Matlab[®] custom-written algorithm as previously described.²³ Mean APD₈₀ was calculated as the average for all pixels in the field of view.

Histological analysis

RV hypertrophy was assessed based on Fulton's Index (RV mass/[LV + septal mass]). Formalin-fixed heart samples were processed with standard paraffin-embedding procedures, cut at 6-µm thickness, and stained with Masson's Trichrome. Images were analysed (blinded to rat group) to quantify fibrous-tissue area (excluding blood vessels, perivascular tissue, and endocardial/epicardial surface) with Image Pro Premier 9.3 Software (MediaCybernetics, MD). Lung samples were fixed and stained with Masson's Trichrome, to analyse pulmonary artery medial wall thickness. Immunohistochemical analyses were performed to identify pro- and anti-inflammatory macrophages (M1 and M2), respectively immunolabelled by CD68 antibody (diluted 1:1000) and CD206 antibody (diluted 1:750). Myeloperoxidase (MPO) antibody (diluted 1:200) was also used to quantify neutrophil invasion in the atria (excluding the circulating neutrophils). Images were analysed, blinded to rat group, for quantification of these inflammation-related cells, with Image Pro Premier 9.3 Software (MediaCybernetics, MD). Counts of the targeted inflammation-

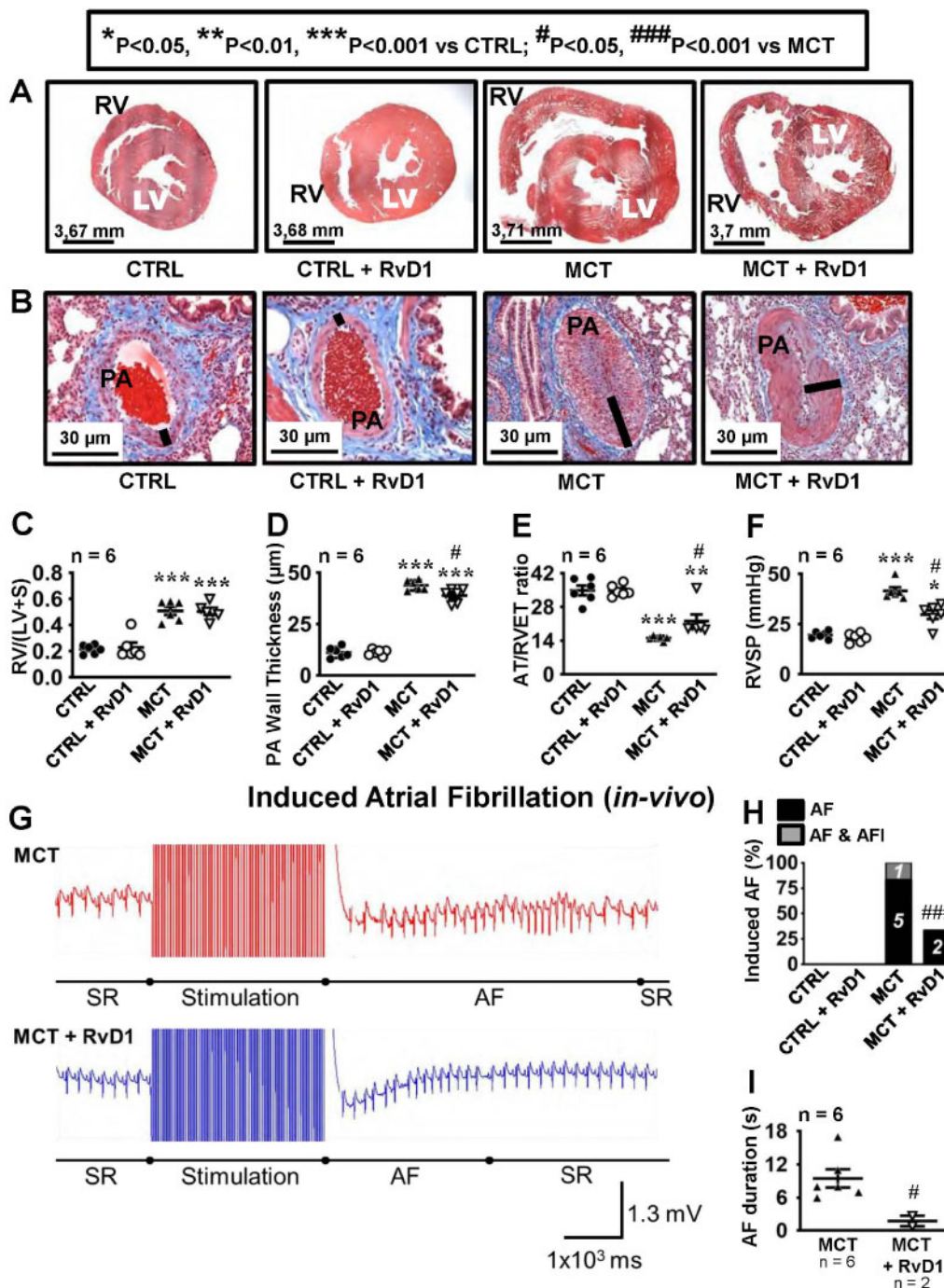


Figure 1 Cardiovascular remodelling and atrial arrhythmia inducibility *in vivo*. (A) Morphometric analyses of the right and left ventricle after 21 days of treatment under control, monocrotaline (MCT) and RvD1 (without and with MCT). (B) Representative lung tissue sections (stained with Masson's Trichrome). Dark lines indicate pulmonary artery wall thickness. (C) Right ventricular (RV) hypertrophy index [ratio of right ventricular (RV) weight over left ventricular + septum (LV + S) weight]. (D) Quantitative analyses of pulmonary artery (PA) wall thickness. (E) Pulmonary artery flow expressed as a ratio of the acceleration time (AT) over the right ventricular ejection time (RVET). (F) Right ventricular pressure (RVSP). All measurements were obtained on Day 21 or on samples taken on Day 21. Results in C–F are mean \pm SEM. (Statistical analysis: one-way ANOVA followed by Bonferroni correction. Each point represents results from an individual animal. $n = 6$ rats per group.) (G) Representative ECGs showing sinus rhythm (SR), 3s burst stimulation and an induced atrial fibrillation (AF) episode in an MCT and in an MCT + RvD1 rat. AF episodes were followed by spontaneous restoration of sinus rhythm. (H) Number of rats that showed AF and AFI during transesophageal EPS *in vivo*. (I) Dot-plot graphs showing mean \pm SEM of AF duration in MCT and MCT + RvD1 treated rats. (Statistical analysis: one-way ANOVA followed by Bonferroni correction. Each point represents results from an individual animal.)

related cells were quantified by an observer blinded to group identity, as the number of cells/mm².

PCR

Tissue samples were freshly isolated, snap-frozen in liquid nitrogen and homogenized in QIAzol[®] Lysis Reagent. Extraction of RNAs was performed with RNeasy[®] Mini Kit (QIAGEN group, Montreal, QC, Canada). RT-PCR was performed with Applied Biosystems Thermal Cycler 2720 (ThermoFisher Scientific, Waltham, MA, USA). Taqman probes were used for collagen1 α 1 (*Col1a1* Rn01463848_m1), collagen3 α 1 (*Col3a1* Rn01437681_m1), α -SMA (*Acta1* Rn01426628_g1), interleukin 6 (*Il6* Rn01410330_m1); and SYBR green primers for glyceraldehyde-3-phosphate dehydrogenase (*Gapdh*), inducible nitric oxide synthase (*Nos2*, iNOS), interleukin-1 β (*Il1 β*), matrix metalloproteinase-2 and -9 (*Mmp2* and *Mmp9*), platelet-derived growth factor receptor alpha and beta (*Pdgfra* and *Pdgfrb*), transforming growth factor beta 1 (*Tgfb1*), and periostin (*Postn*) (Supplementary material online, Table S1).

Gene microarray analysis

Isolation of mRNAs was performed with the Macherey Nagel Nucleospin RNA II isolation kit (Macherey-Nagel Düren, Germany). RNA concentrations were determined with an ND-2000 spectrophotometer (Thermo Fisher Scientific, Waltham, MA, USA), and RNA quality was assessed using an Agilent Bioanalyzer RNA-chip (Agilent, Santa Clara, CA, USA). RNA Integrity Number (RIN) >7 was required for use. Samples from six rats were analysed per experimental group. Samples were pooled pairwise to reduce variability. Transcriptome profiling was obtained with the Affymetrix rat Clariom S Assay including >22 000 gene transcripts (Affymetrix, Santa Clara, CA, USA). Samples were processed on a GeneChip Scanner 3000 7G System (Thermo Fisher Scientific, Waltham, MA, USA).

Quality control and differentially expressed genes were assessed with Transcriptome Analysis Console (TAC) 4.0. The significance filter was set at $P < 0.05$ with a fold-change >2 needed for further analysis. KOBAS 3.0 web server was used for enrichment analysis to determine signalling pathways.^{24,25} DAVID database was used to analyse biological process, cellular component, and molecular function.²⁶

Western blot

Proteins were separated by electrophoresis on 4–20% sodium dodecyl sulfate-polyacrylamide gels and transferred electrophoretically onto polyvinylidene difluoride membranes. Tris-buffered saline (TBS) containing 0.2% (volume/volume) Tween-20 and 5% (weight/volume) bovine serum albumin (BSA) were used to block the membranes. Membranes were then incubated overnight at 4°C with primary antibodies diluted in TBS containing 0.2% Tween-20 and 1% BSA. Membranes were washed with TBS-Tween/1% BSA and hybridized with horseradish peroxidase-conjugated secondary antibody. Detection of immunoreactive bands was performed by electrochemiluminescence with BioMax films (Sigma-Aldrich, San Luis, MO, USA). Protein levels were quantified with Quantity One software (Bio-Rad, Hercules, CA, USA). All expression data were relative to glyceraldehyde-3-phosphate dehydrogenase (GAPDH) staining for the same samples on the same gels.

Drugs and chemical reagents

MCT was obtained from Sigma-Aldrich (St. Louis, MO, USA). Resolvin D1 was obtained from Cayman Chemical (Ann Arbor, MI, USA). Blebbistatin and di-4-ANEPPS were obtained from Cedarlane (Burlington, Ontario, Canada). ACTA1, COL1 α 1, COL3 α 1, GAPDH, IL1 β , IL6, iNOS (*Nos2*), MMP2, MMP9, PDGFR α , PDGFR β , POSTN and TGF β 1 qPCR probes, as well as CD68 and MPO polyclonal antibodies, were obtained from Thermo Fisher Scientific (Waltham, MA). CD206 polyclonal antibody was obtained from Abcam (Toronto, Ontario, Canada).

Antibodies used for western blot experiments included: CASP1 (SC-56036 monoclonal) obtained from Santa Cruz (Texas, DA, USA); GAPDH

(10R-G109a monoclonal) obtained from Fitzgerald (North Acton, MA, USA); α -SMA (ab92536 polyclonal), COL1A1 (ab34710 polyclonal) and MMP2 (ab92536 monoclonal) obtained from Abcam (Toronto, Ontario, Canada); ASC (NBP1-78977 polyclonal), COL3A1 (NB600-594 polyclonal) and NLRP3 (NBP1-77080SS polyclonal) obtained from Novus Biologicals (Centennial, CO, USA), CXCL1 (PA1-29220 polyclonal), CXCL2 (PA5-88673 polyclonal), IL1 β (PA5-46956 polyclonal), IL6 (ARC0962 monoclonal), CASP8 (MA5-15914 monoclonal) and TGF β 3 (PA551070 polyclonal) obtained from Thermo fisher (Waltham, MA, USA).

Data analysis and statistics

The Student's *t*-test (for two-sample analyses only) or one-way or two-way analysis of variance (ANOVA) was performed for statistical analysis. ANOVA followed by *post hoc* Tukey or Bonferroni-corrected Student's *t*-tests were performed to evaluate group differences when analyses of variance revealed significant group effects. Shapiro–Wilk tests were performed to assess consistency with normal distribution. The Fisher's exact test was used for categorical variables like AF inducibility. Results are expressed as mean \pm SEM (standard error of the mean). Statistically significant differences were defined as two-tailed *P*-values <0.05.

Results

Effect of RvD1 on MCT-induced cardiac structural and functional remodelling

MCT caused substantial pulmonary vascular and right heart remodelling. Figures 1A and B shows histological sections of heart and lung tissue from control, control + RvD1, MCT, and MCT + RvD1 rats, obtained 21 days after injection. The RV was hypertrophied and dilated in both MCT-treated groups (Figure 1A). Fulton's index (RV mass normalized to left ventricle + septal mass) was significantly increased from 0.22 ± 0.01 (control) to 0.51 ± 0.03 in MCT-rats. Histological analysis showed that RvD1 did not affect RV structure, whether in control or MCT conditions (Figure 1A and C).

Pulmonary artery (PA) wall thickness increased significantly in MCT-rats (to $43.8 \pm 1 \mu\text{m}$) vs. controls ($11.2 \pm 1.1 \mu\text{m}$). RvD1 treatment did not affect control PA wall thickness under control conditions, and slightly (by about 11%) but significantly reduced PA wall thickness in the presence of MCT, indicating slight attenuation of PA remodelling (Figure 1B and D). PA flow, as assessed by acceleration time to right ventricular ejection time (AT/RVET) ratio, was significantly decreased in MCT-rats (to 15.1 ± 0.4) vs. controls (34.8 ± 2). RvD1 did not influence PA flow under control conditions; however, it slightly but significantly attenuated the effect of MCT (Figure 1E). RVSP more than doubled under MCT treatment (Figure 1F). RvD1 had no effect on RVSP under control conditions; however, RvD1 treatment attenuated MCT-enhanced RVSP by about 30%.

On echocardiography, RvD1 had no effect in control conditions. MCT-rats showed decreased right ventricular systolic contractility compared to control; RvD1 did not prevent this functional remodelling (Supplementary material online, Figure S1A). All MCT-rats showed decreased TAPSE (Supplementary material online, Figure S1B) and tricuspid annulus motion velocity (Supplementary material online, Figure S1C). RvD1 attenuated the effects on TAPSE, without significantly altering tricuspid annulus motion velocity. Tricuspid regurgitation was also observed in rats with RHD; RvD1 did not prevent this dysfunction (Supplementary material online, Figures S1D, S2, and Online Videos). LV parameters showed slight reduction in LV dimensions and augmentation in LV ejection fraction in MCT treated rats. RvD1 normalized changes in

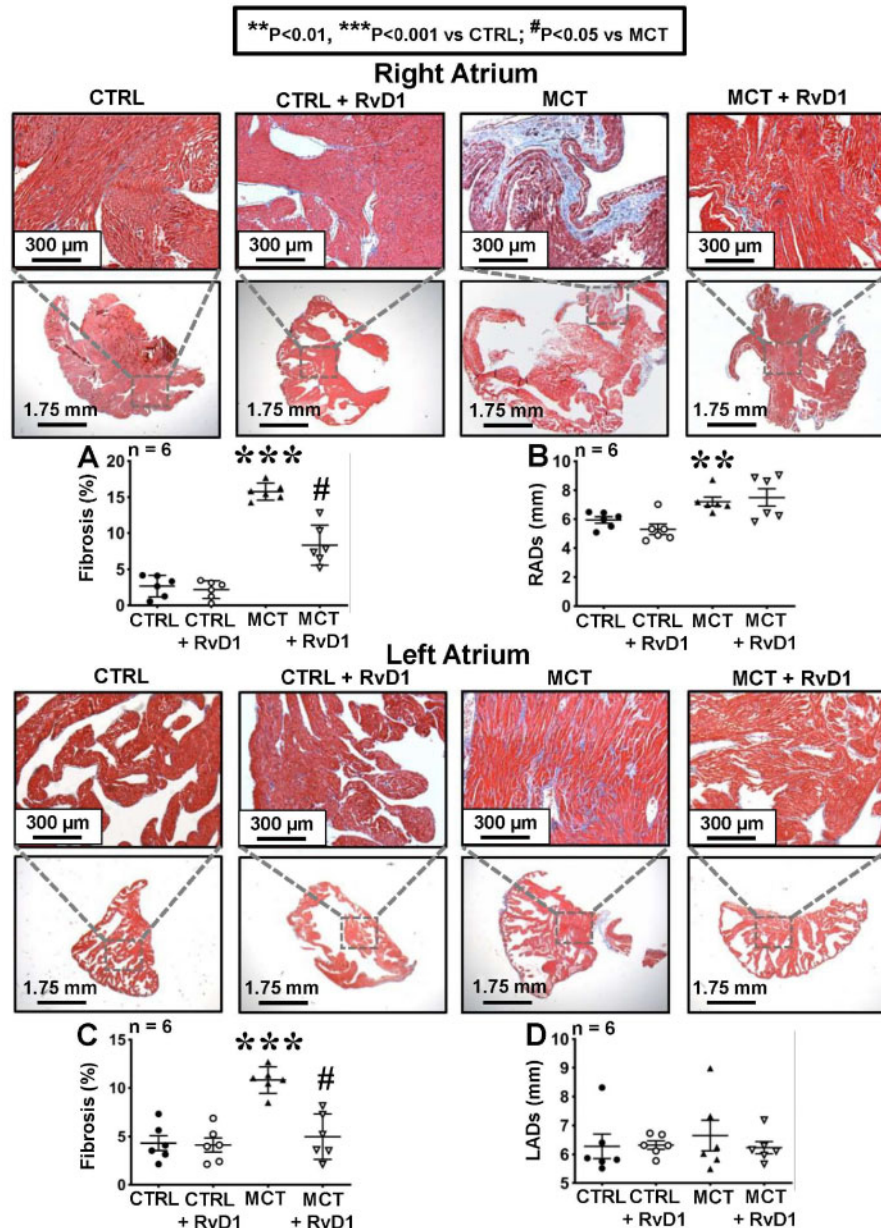


Figure 2 Fibrosis quantification. Histological analysis of right (upper panels) and left (lower panels) atria stained with Masson's Trichrome 21 days after treatment under control, MCT-, and RvD1 ± MCT conditions. (A) Percentage RA fibrotic area and (B) RA dimension at the end of systole (RADs). (C) Percentage LA fibrotic area and (D) LA dimension at the end of systole (LADs). Results in A–D are mean ± SEM. (Statistical analysis: one-way ANOVA followed by Bonferroni correction. Each point represents results from an individual animal. $n = 6$ rats per group.)

aortic blood pressure, LV anterior wall at end-diastole (LVAWd) and LV ejection fraction (Supplementary material online, Table S2). Overall, RvD1 had small, if any, protective effects against MCT-induced PA and RV remodelling.

Effects of RvD1 on MCT-induced AF vulnerability and ECG modifications *in vivo*

Transoesophageal stimulation (Figure 1G) failed to induce AF in control rats, but induced AF in all MCT-only rats (Figure 1H). One MCT rat also developed runs of AFL in addition to AF. In the presence of MCT-

induced remodelling, RvD1 produced a significant (67%) decrease in AF inducibility (Figure 1H). RvD1 also significantly decreased mean AF duration in MCT + RvD1 rats (Figure 1I).

Analysis of ECG variables showed that MCT increased P-wave duration (Supplementary material online, Figure S3A), R–R (Supplementary material online, Figure S3B), and QT intervals (Supplementary material online, Figure S3C), while QRS duration was decreased (Supplementary material online, Figure S3D) and PR interval was unchanged (Supplementary material online, Figure S3E). RvD1 had no effect on control electrocardiograms (ECGs), but significantly attenuated all ECG alterations associated with MCT treatment.

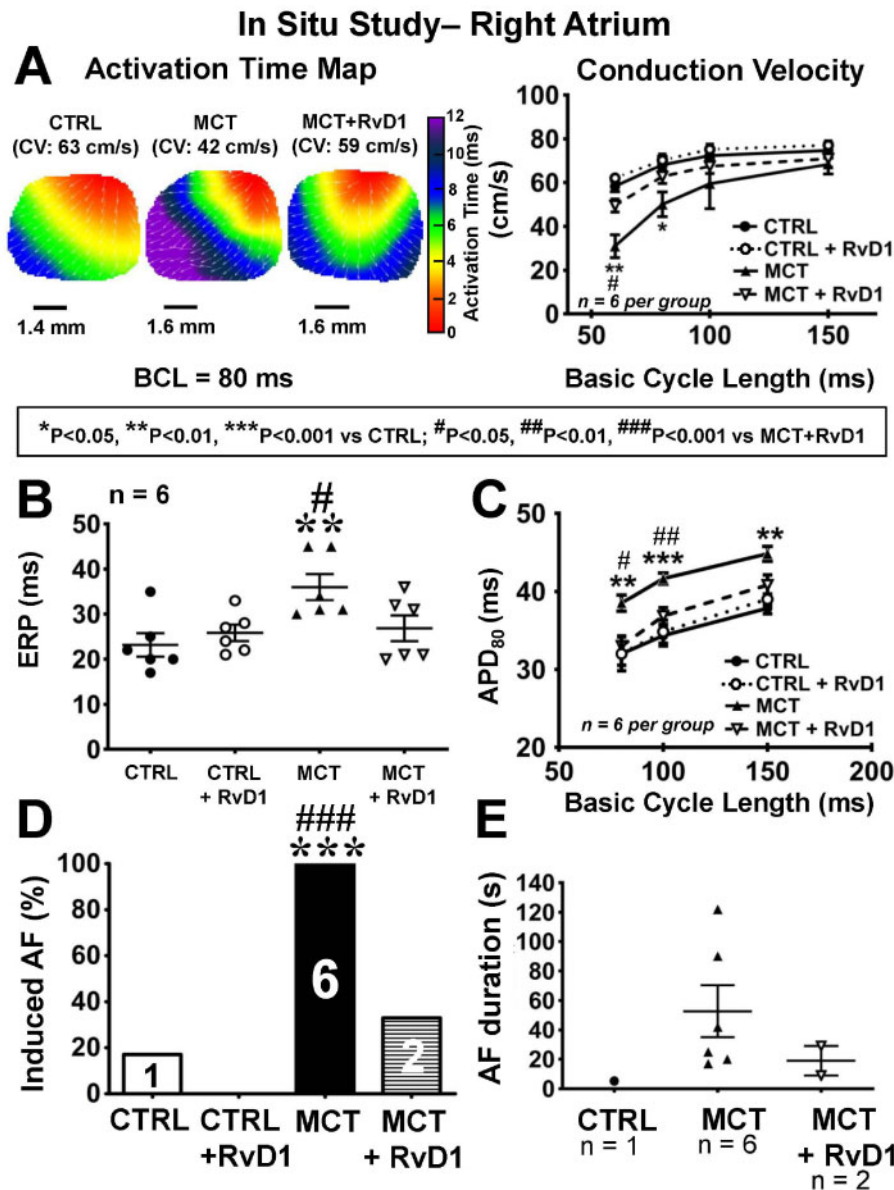


Figure 3 Right atrial optical mapping. (A) Left: right-atrial (RA) activation maps at BCL 80 ms. Right: mean \pm SEM RA conduction velocity values. (B) RA effective refractory period (mean \pm SEM). (C) Action potential duration at 80% repolarization (APD₈₀, mean \pm SEM). (D) Number of rats/group (of 6/group) with AF induced by RA programmed stimulation. (E) AF mean duration (\pm SEM). (Statistical analysis: A and C: two-way ANOVA followed by Tukey's test. B, C, and E: one-way ANOVA followed by Bonferroni correction. D: the Fisher's exact test. Each point in B and E represents results from an individual animal. n = 6 rats per group.)

Effects of RvD1 on RHD-associated atrial structural remodelling

Atrial fibrosis is a common theme for a wide range of AF substrates,²⁷ and prominently figures in the pathophysiology of AF in RHD.^{9,28} RA fibrous-tissue content was significantly increased about five-fold in MCT-rats (Figure 2A). In addition, RA dilation occurred in MCT-treated rats (Figure 2B). RvD1 significantly reduced RA fibrosis (by over 50%) in MCT-exposed rats (Figure 2A) without preventing RA dilation (Figure 2B). In the left atrium, MCT increased fibrous-tissue content over two-fold (Figure 2C) without LA dilation (Figure 2D). RvD1 treatment prevented MCT-induced LA fibrosis (Figure 2C).

RvD1 effects on RHD-associated atrial electrophysiological changes *in situ*

RA CV was slowed in MCT rats, with slowing increasing at shorter BCLs (Figure 3A). RA ERP (Figure 3B) and APD₈₀ (Figure 3C) were significantly increased in MCT rats compared to control. CV was slowed in left atrium to a somewhat lesser, but still significant, extent compared to RA changes in MCT-rats (Supplementary material online, Figure S4A). LA ERP (Supplementary material online, Figure S4B) and APD (BCL 80) (Supplementary material online, Figure S4C) also significantly increased with MCT-only.

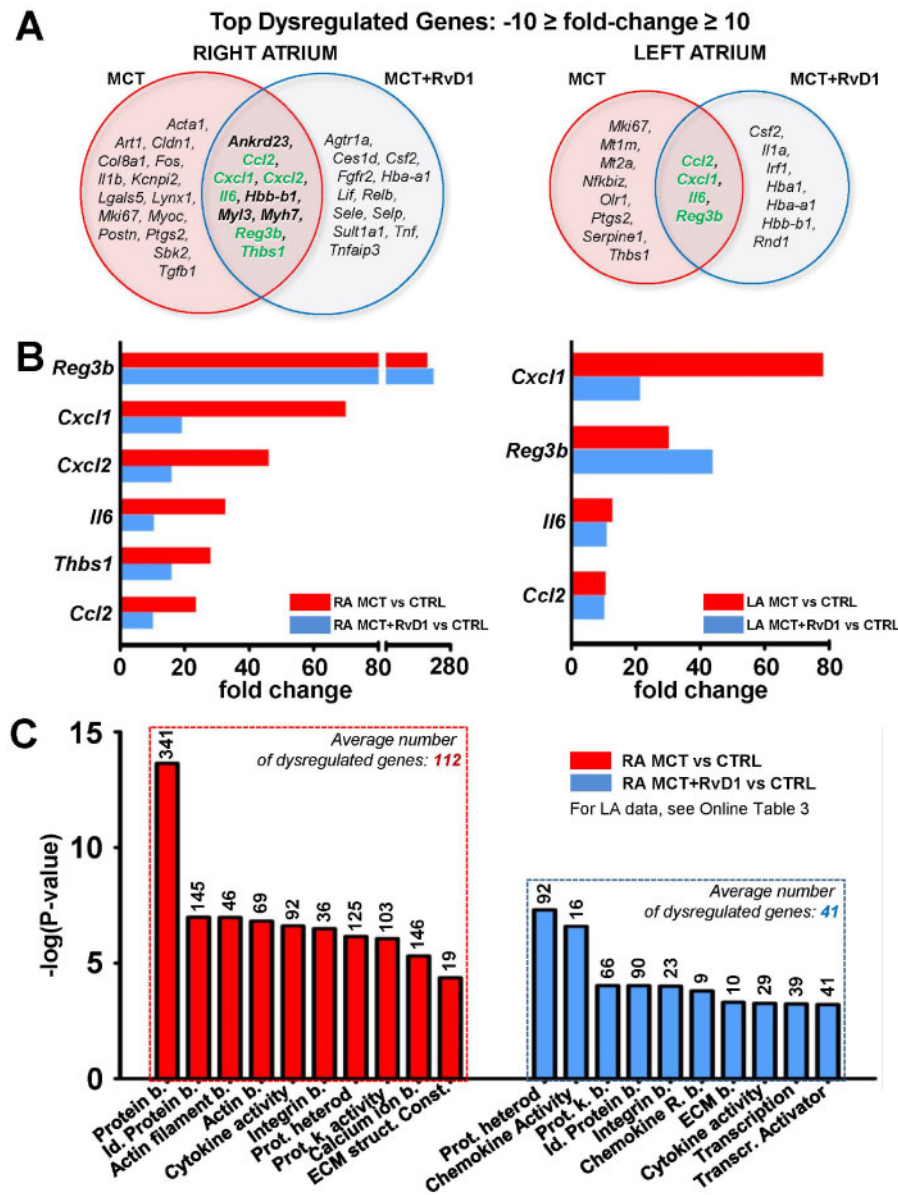


Figure 4 Top dysregulated genes and ontology classification. (A) Venn diagrams of the top dysregulated genes ($-10 \geq \text{fold-change} \geq 10$) under MCT (red) and MCT + RvD1 (blue) compared to control in RA (left panel) and LA (right panel). Commonly dysregulated genes in MCT and MCT + RvD1 related to inflammation are in green. (B) Top common differentially expressed inflammation-related genes in MCT compared to control and MCT + RvD1 treatment compared to control, in RA (left panel) and LA (right panel). (C) Molecular functions dysregulated under MCT vs. control (left, red bars) and MCT + RvD1 treatment vs. control (right, blue bars). Bars show statistical significance of differentially expressed genes and associated numbers indicate the number of dysregulated genes ($n = 6$ rats/group; $P < 0.05$). b., binding; Const., constituent; ECM, extracellular matrix; heterod., heterodimerization; Id., identical; k., kinase; Prot., protein; R., receptor; Transcr., transcription.

RvD1 treatment prevented the electrophysiological changes caused by MCT, maintaining CV, ERP and APD in the range of control values (Figure 3 and Supplementary material online, Figure S4). Consistent with the results of *in vivo* EPSs, *in situ* atrial burst-pacing (Supplementary material online, Table S3) revealed that AF inducibility was significantly increased in right atrium (Figure 3D) under MCT-only conditions (6/6) vs. control (1/6); RvD1 significantly attenuated AF inducibility under MCT

conditions. Qualitatively similar results were seen for programmed stimulation in left atrium (Supplementary material online, Figure S4D). AF duration was quantitatively larger in MCT vs. control rats, and shorter in MCT + RvD1 rats vs. MCT-only, but perhaps because of the small numbers ($n = 1$ inducible control rat, $n = 2$ inducible MCT + RvD1 rats), the differences were not statistically significant (Figure 3E, Supplementary material online, Figure S4E).

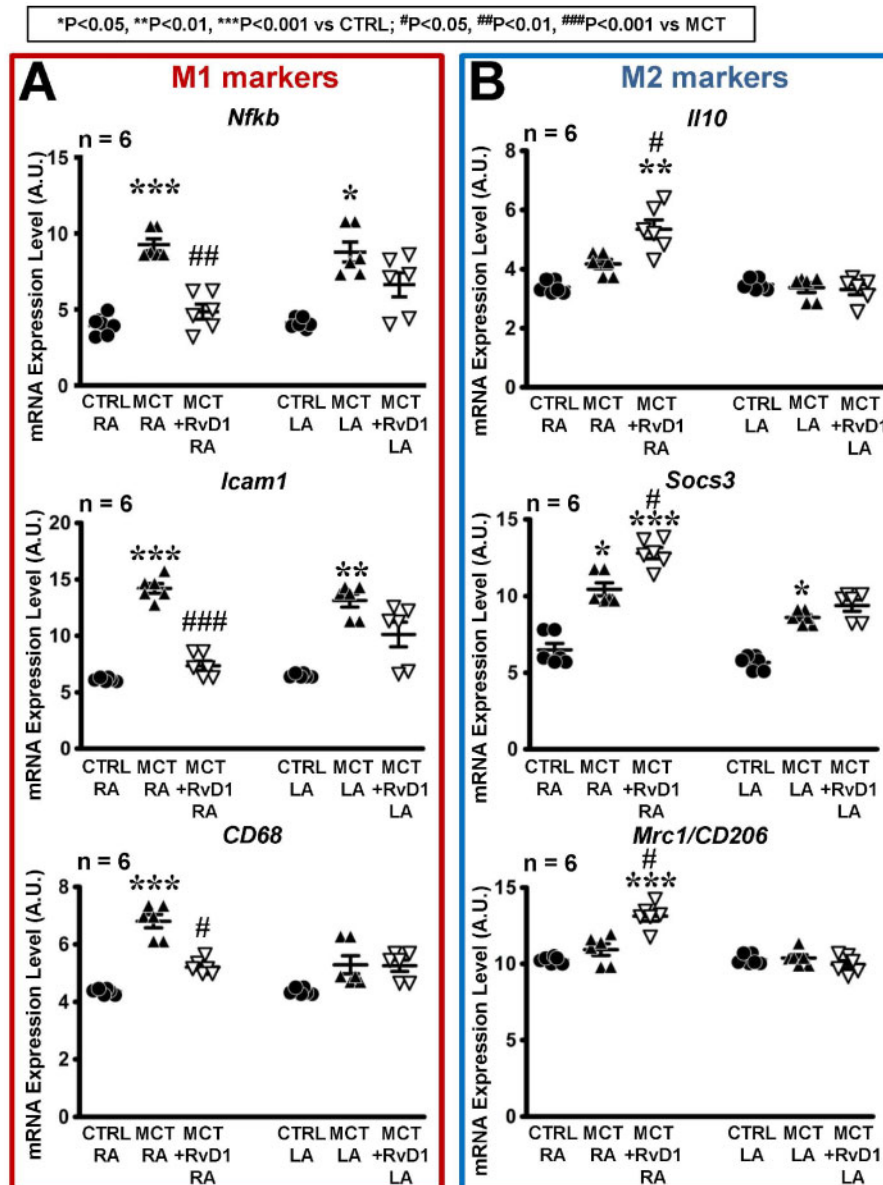


Figure 5 Gene expression of specific macrophage markers. Gene expression level (mean \pm SEM), from pangenomic transcriptome microarray analysis, expressed in arbitrary units (A.U.) for (A) proinflammatory (M1) macrophage markers: *Nfkb*, *Icam1*, *CD68* and (B) anti-inflammatory (M2) macrophage markers: *Il10*, *Socs3*, *Mrc1/CD206*, in RA and LA. (Statistical analysis: one-way ANOVA followed by Bonferroni correction. Each point represents results from an individual animal. $n = 6$ rats per group.)

Effect of RvD1 on expression of selected genes by qPCR

The expression of selected fibrosis-related genes was investigated by qPCR. A variety of important genes, including *Col1a1*, *Col3a1*, *Tgfb1*, *Acta1*, *Mmp2*, and *Pdgfrb* (Supplementary material online, Figure S5) were up-regulated in right atrium of MCT-rats. No statistically significant increases were observed in left atrium of MCT-rats. RvD1 treatment attenuated the MCT-induced up-regulation of these genes, with statistically significant decreases in the right atrium for *Col1a1*, *Col3a1*, and *Mmp2*; and in the left atrium for *Tgfb1*.

Transcriptomic analysis of effects of RvD1 on RHD-activated pathways

We applied pangenomic transcriptome microarray analysis to address the potential molecular pathways mediating the protective effect of RvD1 on MCT-induced remodelling.

KOBAS database analysis indicated that 334 pathways were enriched, with statistically significant differential expression, in the right atrium of MCT-rats vs. control (Supplementary material online, Figure S6). In the right atrium of MCT + RvD1 treated rats a smaller number of pathways (177) was dysregulated vs. control. Among the top 20 dysregulated pathways from each comparison shown in the

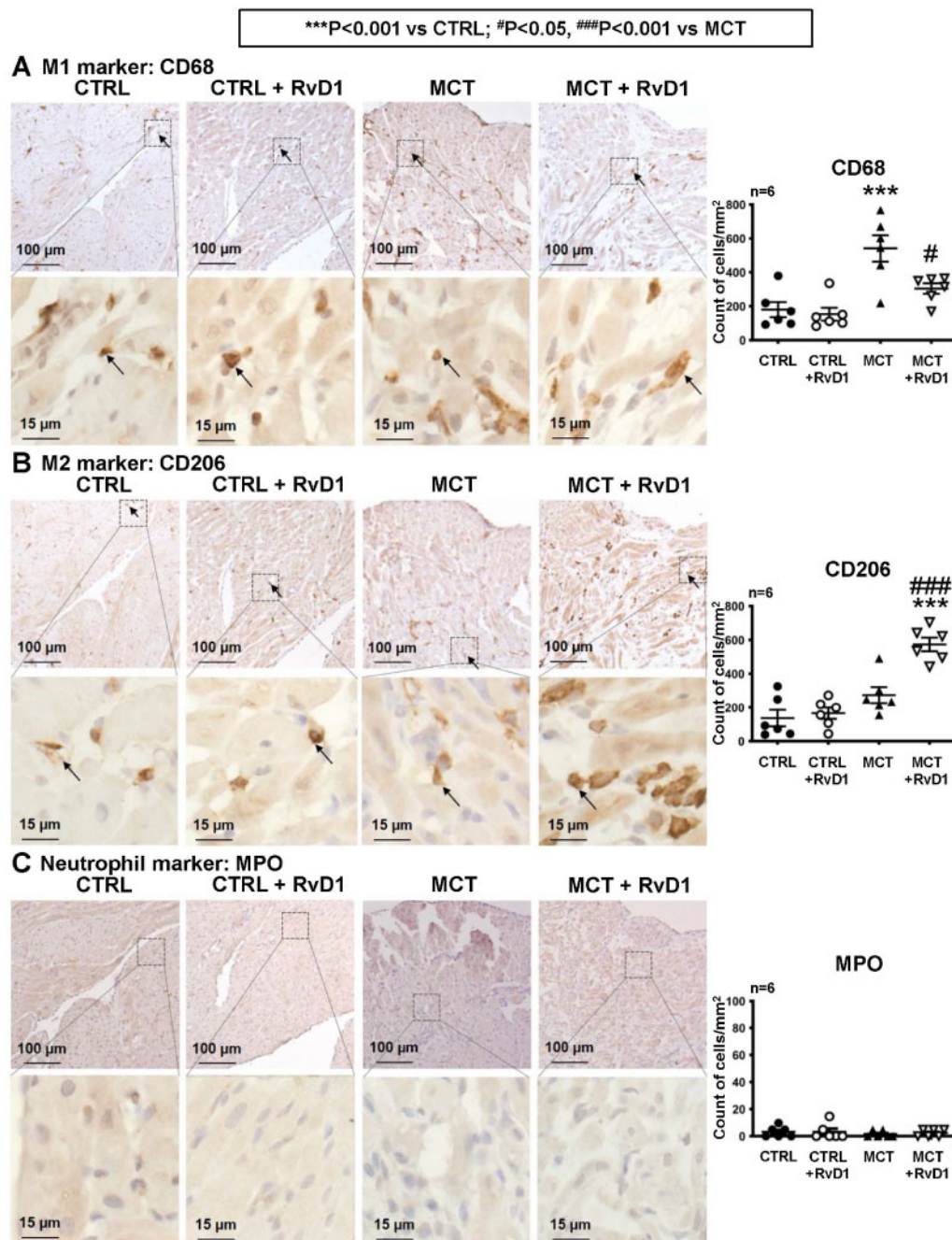


Figure 6 Histological analysis of pro- and anti-inflammatory macrophage infiltration. Immunohistochemical staining (brown coloration) of (A) proinflammatory (M1) macrophage marker CD68, (B) anti-inflammatory (M2) macrophage marker CD206, and (C) neutrophil marker myeloperoxidase (MPO), in right atria. Arrows indicate representative immune-targeted macrophages. Dot-plot graphs show the mean \pm SEM number of right atrial CD68, CD206, and neutrophil cells per mm². (Statistical analysis: one-way ANOVA followed by Bonferroni correction. Each point represents results from an individual animal. $n = 6$ rats per group.)

figure, a majority was related to inflammation and fibrosis. RvD1 notably attenuated changes in inflammation-related pathway genes involved in: advanced glycation end products/receptors (AGE-RAGE), TGF β , mitogen-activated protein kinase (MAPK), and/or phosphatidylinositol 3-kinases-protein kinase B (PI3k-AKT) signalling, as well as focal adhesion and cytokine signalling pathways central in extracellular matrix (ECM) regulation and fibrosis development.

To better understand the relation between these pathways and the pathophysiology of RHD and RvD1 effects, we analysed the expression changes of the most dysregulated genes. Figure 4A shows Venn diagrams of the most statistically significant differentially expressed genes under MCT-only and MCT + RvD1 vs. control in the right and the left atrium. Among the top dysregulated genes commonly expressed in MCT and MCT + RvD1 compared to control, six were related to inflammation

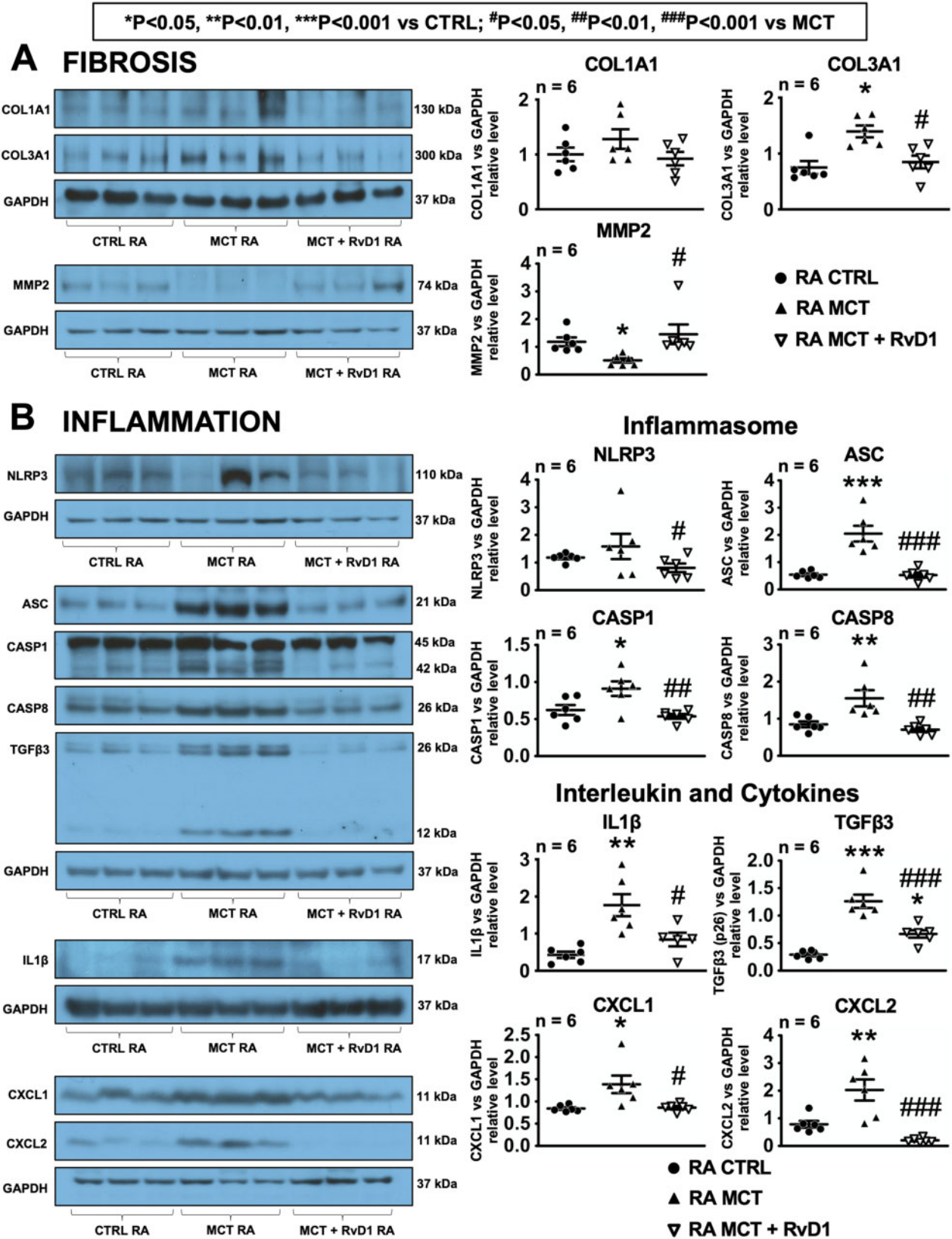


Figure 7 Protein expression of fibrosis- and inflammation-related genes. Western blot analysis of (A) fibrosis-related proteins: COL1A1, COL3A1, and MMP2 and (B) effectors of inflammation: NLRP3, ASC, CASP1, CASP8, IL1β, TGFβ3, CXCL1, and CXCL2. Images are grouped according to gels on which they were run, along with corresponding GAPDH bands. (Statistical analysis: one-way ANOVA followed by Bonferroni correction. Each point represents results from an individual animal. n = 6 rats per group.)

and fibrosis [C-C motif chemokine ligand 2 (*Ccl2*), C-X-C motif chemokine ligand 1 (*Cxcl1*), *Cxcl2*, *Il6*, regenerating islet-derived 3 beta (*Reg3b*), and thrombospondin 1 (*Thbs1*); green in the figure]. In the right atrium, RvD1 given to MCT-rats decreased the expression of the cytokines *Ccl2*, *Cxcl1*, *Cxcl2*, *Il6*, and *Thbs1* compared to MCT-only (Figure 4B, left panel). In the left atrium, RvD1 notably decreased the expression of *Cxcl1* compared to MCT-only (Figure 4B, right panel). The DAVID database was used to perform gene ontology classification. MCT-rats treated with RvD1 had fewer differentially expressed genes, at lower levels of statistical significance, than MCT-only rats compared to control (Figure 4C and Supplementary material online, Table S4).

We then focused on the expression of genes involved in arrhythmia-promoting electrical remodelling, encoding connexins, calcium-handling proteins, and ion channel subunits. Gene-microarray data from RA samples revealed that under MCT-only conditions: connexin 43 (*Cx43*), ryanodine receptor 2 (*Ryr2*), sarcoplipin (*Sln*), sodium-calcium exchanger 1 (*Ncx1*), sarco/endoplasmic reticulum Ca^{2+} -ATPase (*Serca*), phospholamban (*Plb*), calcium voltage-gated channel subunit alpha1 C (*Ca α 1c*), potassium voltage-gated channel subfamily (Kcn) A member 1 [*Kcna1*], *Kcna5*, *Kanj2* and *Kanq1* were down-regulated; and *Cx40*, stromal interaction molecule 1 (*Stim1*), calcium release-activated calcium channel protein 1 (*Orai1*), and *Kcna3* were up-regulated vs. control (Supplementary material online, Figure S7). Compared to MCT-only, RvD1-treatment of MCT rats reversed the MCT-effects on *Cx43*, *Ryr2*, *Sln*, *Ncx1*, *Serca*, *Plb*, *Ca α 1c*, *Kcna1*, *Kcna5*, *Kanj2*, and *Kanq1*, consistent with the reversal of electrophysiological changes shown in Figure 3.

Changes in indices of inflammation

There is evidence for a role of inflammation⁷ and specifically the NLRP3 (nucleotide-oligomerization-domain-like receptor family, pyrin domain containing 3) inflammasome¹¹ in AF. The NLRP3-inflammasome-related genes: *Nlrp3*, apoptosis-associated speck-like protein containing caspase recruitment domain (*Asc*), caspase 1 (*Casp1*), *Casp8*, and interleukin 1 beta (*Il1b*) showed increased expression on gene-microarray analysis of MCT-rat RA vs. control (Supplementary material online, Figure S8). MCT-rats receiving RvD1 showed decreased expression of these genes vs. MCT-only, with all but *Asc* showing statistical significance from MCT-only values (Supplementary material online, Figure S8 and Table S4).

To better understand the inflammatory changes produced by MCT-induced RHD with and without RvD1 treatment, we evaluated the expression of markers characterizing proinflammatory type 1 macrophages (M1)- and anti-inflammatory type 2 (M2) macrophages. The gene-expression levels of M1 macrophage markers: nuclear factor kappa-light-chain-enhancer of activated B cells (*Nfkb*), intercellular adhesion molecule 1 (*Icam1*), and cluster of differentiation 68 (*CD68*) were significantly increased on gene-microarray in right atrium of MCT-only rats vs. control (Figure 5A, left); these changes were suppressed by RvD1. LA changes were less striking, but whereas MCT-only significantly enhanced LA expression of *Nfkb* and *Icam1* vs. control, the changes were smaller in RvD1-treated MCT-rats and were not significantly different from control (Figure 5A, right). The M2 markers: interleukin 10 (*Il10*), suppressor of cytokine signalling 3 (*Socs3*), and c-type-mannose-receptor-1/cluster of differentiation 206 (*Mrc1/CD206*) were significantly increased in right atrium of RvD1-treated MCT-rats compared to MCT-only and control rats (Figure 5B).

The gene-expression of effectors of inflammation was evaluated by qPCR. *Postn*, *Il6*, *Il1b*, and *Nos2* were significantly increased in the right and the left atrium of MCT-only compared to control rats. RvD1 treatment reduced the MCT-induced up-regulation of these genes, with MCT + RvD1 rats showing statistically significant decreases relative to MCT-only (Supplementary material online, Figure S9).

Blinded analysis of immunohistological staining of the right atrium from control, MCT and RvD1 rats revealed an increased density of cells expressing the M1 macrophage marker CD68 marker in MCT-only rats vs. control. CD68-expressing M1 macrophage cell number was significantly reduced in RvD1-treated MCT-rat RA vs. MCT-only (Figure 6A). On the other hand, the number of cells expressing the M2-macrophage marker CD206 was significantly increased in MCT-rat RA treated with RvD1 vs. MCT-only or control (Figure 6B). The number of cells expressing the neutrophil-marker myeloperoxidase (MPO) was small in RA tissue (Figure 6C) and did not vary among groups.

Western blot analysis was performed to assess RA levels of proteins involved in fibrosis (COL1A1, COL3A1, MMP2) (Figure 7A), inflammatory (NLRP3, ASC, CASP1, CASP8), interleukin (IL1 β), and cytokines (TGF β 3, CXCL1, and CXCL2) (Figure 7B). MCT rats shown statistically significant increases in protein expression of COL3A1, ASC, CASP1, CASP8, IL1 β , TGF β 3, CXCL1, and CXCL2 compared to control. The protein expression of the collagenase MMP2 was significantly decreased in MCT-only animals compared to control. RvD1 treatment significantly attenuated all MCT-induced protein-expression changes.

Discussion

In this study, we examined the effects of an inflammation-resolution promoting molecule, RvD1, on the development of atrial remodelling and arrhythmogenesis in experimental RHD. RvD1 strongly attenuated atrial fibrotic and electrophysiological remodelling and suppressed AF-promotion, while showing much more modest actions on MCT-induced pulmonary vascular changes and RV remodelling. The improvements in electrophysiology and fibrotic remodelling were associated with marked reductions in inflammation-related gene expression in the presence of RvD1, along with a clear shift in RA macrophage expression away from proinflammatory M1 macrophages and towards M2 macrophages with anti-inflammatory properties.

Right heart disease and AF

RHD is known to be an important potential cause of AF.²⁻⁵ In a large database of Asian subjects, those with AF were over six times as likely as those without AF to have chronic obstructive lung disease.²⁹ The mechanisms underlying the association of AF with RHD have been poorly understood. We recently employed the MCT-induced PH model to study atrial remodelling associated with RHD, finding substantial AF promotion related primarily to atrial fibrotic remodelling.⁹ Prominent inflammatory signalling alterations accompanied the fibrotic changes, so we were motivated to investigate the effect of an intervention promoting the resolution of inflammation. We selected RvD1 based on its low toxicity and recognized anti-inflammatory properties.³⁰

RvD1 and fibrosis

RvD1 is recognized as an endogenous immune responsive, pro-resolving lipid mediator,^{20,21} generated from DHA in response to infection, injury, and inflammation.²⁰ RvD1 has been reported to produce beneficial effects in several experimental disease models. RvD1 inhibits inflammation in a cellular model of Parkinson's disease¹⁸; protects against ischaemia-reperfusion-induced kidney damage and associated fibrosis¹⁷; reduces polymorphonuclear-neutrophil infiltration in periodontitis³⁰; prevents aortic dilation in models of aortic aneurysms³¹; decreases bacterial growth and neutrophil infiltration in cystic fibrosis³²; and prevents cardiorenal syndrome and myocardial infarction-induced LV structural remodelling in myocardial infarction.¹⁶

To our knowledge, ours is the first study examining the effects of RvD1 in a model of RHD or arrhythmia. While we saw prominent anti-fibrotic effects and prevention of arrhythmia susceptibility, the effects on MCT-induced pulmonary vascular changes and RV remodelling were much more modest. These findings suggest that RvD1 does not substantially alter the primary vascular pathophysiology in MCT-induced PH or the RV response, but reduces the inflammation-related alterations that produce the associated atrial changes.

Potential mechanisms of RvD1 effects on RDD-associated AF

RvD1 interacts with the G-coupled protein receptors GPR32 and/or ALX/FPR to produce its actions^{33,34} and can also stimulate the expression of other specialized pro-resolving mediator receptors like ChemR23 (Supplementary material online, Table S5). RvD1 is believed to favour preservation of the ECM by resolving inflammation.³⁵ We noted prominent reductions in a range of inflammatory indicators with RvD1 exposure, accompanying the reductions in atrial fibrosis. RvD1 attenuated the expression of key inflammation-related genes like *Il6*, *Il1b*, *Cd2*, p-selectin (*Selp*), and e-selectin (*Sele*). There is evidence for an important role of the NLRP3 inflammasome in AF.¹¹ We observed substantial increases in the expression of right atrium *Nlrp3*, *Asc*, *Casp1*, *Casp8*, and *Il1b* with MCT-induced RHD (Supplementary material online, Figure S8); these changes were largely reversed by RvD1. Furthermore, whereas MCT caused an accumulation of M1 macrophages (Figures 5A and 6A), RvD1 reversed this trend and produced an increase in M2 macrophages (Figures 5B and 6B). M1 macrophages have a prominent pro-inflammatory phenotype and classically convert the amino acid arginine to bioactive nitric oxide, whereas M2 macrophages have anti-inflammatory effects and convert arginine to ornithine.³⁶ The final profibrotic pathways activated by inflammation were inhibited by RvD1 in our rats, as indicated by significant attenuation of the atrial expression of *Col1a1*, *Col3a3*, *Tgfb1*, *Mmp2*, and *Pdgfrb* (Supplementary material online, Figure S5). RvD1 also exerted inhibitory effects on AGE-RAGE, PI3K-AKT, and MAPK signalling pathways that were enriched by MCT-induced up-regulation of cytokine/chemokine genes like *Il6*, *Cxcl1*, *Cxcl2*, *Ccl2*, and *Thbs1*.

Novel anti-inflammatory and omega-3 fatty acid derivatives in cardiovascular therapeutics

Our observation of the protection provided by RvD1 against RHD-associated atrial arrhythmogenic remodelling adds to a growing list of novel compounds, many derived from omega-3 fatty acids, with therapeutic properties for cardiovascular disease. Icosapent ethyl is a highly purified EPA-derivative that was found to protect against a broad primary cardiovascular endpoint, as well as cardiovascular deaths, in a large randomized multicentre trial (REDUCE-IT) of high-risk patients with heart disease.³⁷ Interestingly, anti-inflammatory actions mediated by RvE1 are one of the main candidates to explain the benefits of icosapent ethyl observed in REDUCE-IT.³⁸ Canakinumab is a monoclonal antibody targeting interleukin 1- β , which has been shown to significantly reduce the rate of cardiovascular events in patients with prior myocardial infarction and elevated blood C-reactive protein concentrations.³⁹ Colchicine, a fairly innocuous and widely used agent with anti-inflammatory properties, has also recently been demonstrated in a large-scale randomized study to prevent myocardial infarction and stroke after an index event.⁴⁰ The field of inflammation-modulating therapeutics for cardiovascular disease appears to be burgeoning, and

our demonstration for the first time of substantial efficacy of an inflammation-resolution promoting molecule in a clinically relevant AF paradigm is of potential importance.

Potential limitations

In this study, we limited ourselves to the specific pathological context of RHD-associated AF. It would be of interest to examine other clinically relevant animal models of AF, such as atrial remodelling associated with heart failure, myocardial infarction and AF-induced remodelling. Since RvD1 is relatively non-toxic, it might be an interesting therapeutic to study in a number of clinical contexts, including the prevention of AF recurrence after ablation. We have only looked at one inflammation-resolving molecule, RvD1, but there is a wide range of agents with varying chemistries, receptor systems and pharmacology that could be investigated.^{14,20,21} Finally, further study of the pharmacokinetics and pharmacodynamics of these agents will be needed to optimize therapeutic dose regimens.

We administered RvD1 on a daily basis after initial dosing with MCT, in order to provide a test in principle of its effectiveness in preventing RHD-associated RA remodelling. The closest analogous clinical situation would be administration immediately after the diagnosis of a RHD-inducing condition like early pulmonary fibrosis or the early stages of chronic obstructive pulmonary disease. Whether the RA pathology due to fully established RHD can be reversed by RvD1 is an interesting question that goes beyond the scope of the present study, but should be explored in future work.

We have studied the MCT model of RHD-related AF because our prior data⁹ pointed to a strong role of inflammatory signalling in the development of the AF substrate. It will be of potential interest to assess the effects of RvD1 therapy in one of the many other animal models of AF.⁴¹

Conclusions

The present study shows that the inflammation-resolution promoting DHA derivative RvD1 attenuates atrial arrhythmogenic remodelling associated with RHD. RvD1 selectively suppressed electrical and fibrotic remodelling in the atria, with little or no effect on RV remodelling. RvD1 is a promising potential lead compound for novel therapeutic approaches to combating atrial arrhythmogenic remodelling in RHD and potentially other conditions.

Data availability

All data underlying this research are available into the article and in its online [supplementary material](#).

Supplementary material

Supplementary material is available at *Cardiovascular Research* online.

Acknowledgements

The authors thank Nathalie L'Heureux, Chantal Saint-Cyr, Cynthia Torok, Marie-Élaine Clavet, and YanFen Shi for their technical assistance; Natacha Duquette and the animal-care staff of the Montreal Heart Institute for their support; Lucie Lefebvre for secretarial assistance with the manuscript; Genome Quebec and Claire Soursou for help with microarray data processing and analysis.

Conflict of interest: none declared.

Funding

This work was supported by the Canadian Institutes of Health Research (CIHR Foundation Grant 148401) and the Heart and Stroke Foundation of Canada (18-0022032).

References

- Andrade J, Khairy P, Dobrev D, Nattel S. The clinical profile and pathophysiology of atrial fibrillation: relationships among clinical features, epidemiology, and mechanisms. *Circ Res* 2014;**114**:1453–1468.
- Goudis CA. Chronic obstructive pulmonary disease and atrial fibrillation: an unknown relationship. *J Cardiol* 2017;**69**:699–705.
- Rajdev A, Garan H, Biviano A. Arrhythmias in pulmonary arterial hypertension. *Prog Cardiovasc Dis* 2012;**55**:180–186.
- Drakopoulou M, Nashat H, Kempny A, Alonso-Gonzalez R, Swan L, Wort SJ, Price LC, McCabe C, Wong T, Gatzoulis MA, Ernst S, Dimopoulos K. Arrhythmias in adult patients with congenital heart disease and pulmonary arterial hypertension. *Heart Br Card Soc* 2018;**104**:1963–1969.
- Wanamaker B, Cascino T, McLaughlin V, Oral H, Latchamsetty R, Siontis KC. Atrial arrhythmias in pulmonary hypertension: pathogenesis, prognosis and management. *Arrhythmia Electrophysiol Rev* 2018;**7**:43–48.
- Heijman J, Algalarrondo V, Voigt N, Melka J, Wehrens XH, Dobrev D, Nattel S. The value of basic research insights into atrial fibrillation mechanisms as a guide to therapeutic innovation: a critical analysis. *Cardiovasc Res* 2016;**109**:467–479.
- Shen MJ, Arora R, Jalife J. Atrial myopathy. *JACC Basic Transl Sci* 2019;**4**:640–654.
- Siebermar J, Kholmovski EG, Marrouche N. Assessment of left atrial fibrosis by late gadolinium enhancement magnetic resonance imaging: methodology and clinical implications. *JACC Clin Electrophysiol* 2017;**3**:791–802.
- Hiram R, Naud P, Xiong F, Al-u'datt D, Algalarrondo V, Sirois MG, Tanguay J-F, Tardif J-C, Nattel S. Right atrial mechanisms of atrial fibrillation in a rat model of right heart disease. *J Am Coll Cardiol* 2019;**74**:1332–1347.
- Harada M, Van Wagoner DR, Nattel S. Role of inflammation in atrial fibrillation pathophysiology and management. *Circ J* 2015;**79**:495–502.
- Yao C, Veleva T, Scott L, Cao S, Li L, Chen G, Jayabal P, Pan X, Alsina KM, Abu-Taha I, Dr, Ghezalbash S, Reynolds CL, Shen YH, LeMaire SA, Schmitz W, Müller FU, El-Armouche A, Tony Eissa N, Beeton C, Nattel S, Wehrens XHT, Dobrev D, Li N. Enhanced cardiomyocyte NLRP3 inflammasome signaling promotes atrial fibrillation. *Circulation* 2018;**138**:2227–2242.
- Zhou X, Dudley SC Jr. Evidence for inflammation as a driver of atrial fibrillation. *Front Cardiovasc Med* 2020;**7**:62.
- Shuai W, Kong B, Fu H, Shen C, Jiang X, Huang H. MD1 deficiency promotes inflammatory atrial remodeling induced by high-fat diets. *Can J Cardiol* 2019;**35**:208–216.
- Serhan CN. Pro-resolving lipid mediators are leads for resolution physiology. *Nature* 2014;**510**:92–101.
- Spite M, Clària J, Serhan CN. Resolvins, specialized proresolving lipid mediators, and their potential roles in metabolic diseases. *Cell Metab* 2014;**19**:21–36.
- Halade GV, Kain V, Serhan CN. Immune responsive resolvin D1 programs myocardial infarction-induced cardiorenal syndrome in heart failure. *FASEB J* 2018;**32**:3717–3729.
- Duffield JS, Hong S, Vaidya VS, Lu Y, Fredman G, Serhan CN, Bonventre JV. Resolvin D series and protectin D1 mitigate acute kidney injury. *J Immunol* 2006;**177**:5902–5911.
- Xu J, Gao X, Yang C, Chen L, Chen Z. Resolvin D1 attenuates Mpp+-induced Parkinson disease via inhibiting inflammation in PC12 cells. *Med Sci Monit* 2017;**23**:2684–2691.
- Levy BD. Resolvin D1 and resolvin E1 promote the resolution of allergic airway inflammation via shared and distinct molecular counter-regulatory pathways. *Front Immunol* 2012;**3**:390.
- Serhan CN. Treating inflammation and infection in the 21st century: new hints from decoding resolution mediators and mechanisms. *FASEB J* 2017;**31**:1273–1288.
- Pirault J, Bäck M. Lipoxin and resolvin receptors transducing the resolution of inflammation in cardiovascular disease. *Front Pharmacol* 2018;**9**:1273.
- Reil J-C, Hohl M, Selezan S, Lipp P, Drautz F, Kazakow A, Münz BM, Müller P, Steendijk P, Reil GH, Allessie MA, Böhm M, Neuberger HR. Aldosterone promotes atrial fibrillation. *Eur Heart J* 2012;**33**:2098–2108.
- Xiong F, Qi X, Nattel S, Comtois P. Wavelet analysis of cardiac optical mapping data. *Comput Biol Med* 2015;**65**:243–255.
- Wu J, Mao X, Cai T, Luo J, Wei L. KOBAS server: a web-based platform for automated annotation and pathway identification. *Nucleic Acids Res* 2006;**34**:W720–W724.
- Xie C, Mao X, Huang J, Ding Y, Wu J, Dong S, Kong L, Gao G, Li CY, Wei L. KOBAS 2.0: a web server for annotation and identification of enriched pathways and diseases. *Nucleic Acids Res* 2011;**39**:W316–W322.
- Huang DW, Sherman BT, Lempicki RA. Systematic and integrative analysis of large gene lists using DAVID bioinformatics resources. *Nat Protoc* 2009;**4**:44–57.
- Nattel S, Burstein B, Dobrev D. Atrial remodeling and atrial fibrillation: mechanisms and implications. *Circ Arrhythm Electrophysiol* 2008;**1**:62–73.
- Medi C, Kalman JM, Ling L-H, Teh AW, Lee G, Lee G, Spence SJ, Kaye DM, Kistler PM. Atrial electrical and structural remodeling associated with longstanding pulmonary hypertension and right ventricular hypertrophy in humans. *J Cardiovasc Electrophysiol* 2012;**23**:614–620.
- Li YG, Pastori D, Farcomeni A, Yang PS, Jang E, Joung B, Wang YT, Guo YT, Lip G. A simple clinical risk score (C₂HES_T) for predicting incident atrial fibrillation in Asian subjects: derivation in 471,446 Chinese subjects, with internal validation and external application in 451,199 Korean subjects. *Chest* 2019;**155**:510–518.
- Sun Y-P, Oh SF, Uddin J, Yang R, Gotlinger K, Campbell E, Colgan SP, Petasis NA, Serhan CN. Resolvin D1 and its aspirin-triggered 17 R epimer. Stereochemical assignments, anti-inflammatory properties, and enzymatic inactivation. *J Biol Chem* 2007;**282**:9323–9334.
- Spinosa M, Su G, Salmon MD, Lu G, Cullen JM, Fashandi AZ, Hawkins RB, Montgomery W, Meher AK, Conte MS, Sharma AK, Ailawadi G, Upchurch GR Jr. Resolvin D1 decreases abdominal aortic aneurysm formation by inhibiting NETosis in a mouse model. *J Vasc Surg* 2018;**68**:935–1035.
- Philippe R, Urbach V. Specialized pro-resolving lipid mediators in cystic fibrosis. *IJMS* 2018;**19**:2865.
- Krishnamoorthy S, Recchiuti A, Chiang N, Fredman G, Serhan CN. Resolvin D1 receptor stereoselectivity and regulation of inflammation and proresolving microRNAs. *Am J Pathol* 2012;**180**:2018–2027.
- Kain V, Ingle KA, Colas RA, Dalli J, Prabhu SD, Serhan CN, Joshi M, Halade GV. Resolvin D1 activates the inflammation resolving response at splenic and ventricular site following myocardial infarction leading to improved ventricular function. *J Mol Cell Cardiol* 2015;**84**:24–35.
- Zheng S, Wang Q, D'Souza V, Bartis D, Dancer R, Parekh D, Gao F, Lian Q, Jin S, Thickett DR. ResolvinD1 stimulates epithelial wound repair and inhibits TGF-β-induced EMT whilst reducing fibroproliferation and collagen production. *Lab Invest* 2018;**98**:130–140.
- Mills CD. Anatomy of a discovery: M1 and M2 macrophages. *Front Immunol* 2015;**6**:212.
- Bhatt DL, Steg PG, Miller M, Brinton EA, Jacobson TA, Ketchum SB, Doyle RT, Juliano RA, Jiao L, Granowitz C, Tardif J-C, Ballantyne CM; REDUCE-IT Investigators. Cardiovascular risk reduction with icosapent ethyl for hypertriglyceridemia. *N Engl J Med* 2019;**380**:11–22.
- Bäck M, Hansson GK. Omega-3 fatty acids, cardiovascular risk, and the resolution of inflammation. *FASEB J* 2019;**33**:1536–1539.
- Ridker PM, Everett BM, Thuren T, MacFadyen JG, Chang WH, Ballantyne C, Fonseca F, Nicolau J, Koenig W, Anker SD, Kastelein JJP, Cornel JH, Pais P, Pella D, Genest J, Cifkova R, Lorenzatti A, Forster T, Kobalava Z, Vida-Simiti L, Flather M, Shimokawa H, Ogawa H, Dellborg M, Rossi PRF, Troquay RPT, Libby P, Glynn RJ; CANTOS Trial Group. Antiinflammatory therapy with canakinumab for atherosclerotic disease. *N Engl J Med* 2017;**377**:1119–1131.
- Tardif J-C, Kouz S, Waters DD, Bertrand OF, Diaz R, Maggioni AP, Pinto FJ, Ibrahim R, Gamra H, Kiwan GS, Berry C, López-Sendón J, Ostadal P, Koenig W, Angoulvant D, Grégoire JC, Lavoie M-A, Dubé M-P, Rhoads D, Provencher M, Blondeau L, Orfanos A, L'Allier PL, Guertin M-C, Roubille F. Efficacy and safety of low-dose colchicine after myocardial infarction. *N Engl J Med* 2019;**381**:2497–2505.
- Nishida K, Michael G, Dobrev D, Nattel S. Animal models for atrial fibrillation: clinical insights and scientific opportunities. *Europace* 2010;**12**:160–172.

Translational perspective

Mounting evidence suggests that chronic diseases are promoted by failure of inflammation to resolve. Here, we tested the effects of a molecule that promotes inflammation-resolution, Resolvin-D1, in a rat model of atrial arrhythmogenic remodelling caused by right-heart disease and marked by signs of persistent inflammatory signalling. Resolvin-D1 suppressed inflammatory signalling, shifted the balance of atrial macrophage-infiltration from proinflammatory M1 macrophages towards anti-inflammatory M2-macrophages and prevented atrial fibrosis. Disease-induced conduction-slowness was suppressed and atrial fibrillation promotion was prevented. These findings support the potential value of a relatively non-toxic inflammation-resolving molecule in preventing the development of an arrhythmogenic substrate associated with chronic inflammatory signalling.